



Conference Paper

**HEAT TRANSFER MODES IN
SUPERCRITICAL FLUIDS**

COMPANY WIDE

CW-125100-CONF-003

Revision 0

Prepared by
Rédigé par

Reviewed by
Vérifié par

Approved by
Approuvé par

2012/11/27

UNRESTRICTED

2012/11/27

ILLIMITÉ

©Atomic Energy of
Canada Limited

Chalk River, Ontario
Canada K0J 1J0

©Énergie Atomique du
Canada Limitée

Chalk River (Ontario)
Canada K0J 1J0

HEAT TRANSFER MODES IN SUPERCRITICAL FLUIDS

Sun-Kyu Yang

Chalk River Laboratories, Atomic Energy of Canada Limited, Chalk River, Ontario, K0J 1J0,
Canada

yangsk@aecl.ca

ABSTRACT

The Canadian SCWR (supercritical water-cooled reactor), which operates at supercritical pressure and temperature, is being developed at AECL. It is required that flow and heat-transfer characteristics at supercritical conditions be investigated. The heat-transfer modes in supercritical fluids were studied using heat-transfer data from supercritical CO₂ flow. Entrance-affected, normal and deteriorated heat transfer were defined using CO₂ data from upward flow in an 8 mm diameter tube. The threshold value for normal heat transfer was defined using normal and deteriorated heat-transfer data. Normal and deteriorated heat transfer correlations were separately derived using the relevant data. The correlations developed include the effect of flow condition parameters on heat transfer for different heat-transfer modes.

1. INTRODUCTION

The Canadian SCWR, which operates at supercritical pressure and temperature, is being developed at AECL [1]. It is important to understand flow and heat-transfer characteristics to evaluate thermal performance at supercritical conditions [2].

The heat transfer in supercritical fluids is usually categorized into two modes; which are normal and deteriorated heat transfer. It is difficult to define these different modes when analyzing experimental data because they are often not differentiated clearly due to the data scatter. As a consequence, heat-transfer correlations are sometimes derived from the combined data of all heat-transfer modes due to the difficulty in separating the heat transfer mode. This is not an appropriate approach because the deteriorated heat transfer is not included in the thermal-performance evaluation for supercritical conditions.

Thus, it is required to differentiate the heat transfer mode with a more systematic criterion, and to understand characteristics for different heat-transfer modes. The heat-transfer modes in supercritical fluids were investigated using heat-transfer data from supercritical CO₂ flow. CO₂ is one of the modeling fluids that are used to simulate water at supercritical conditions [2]. Replacing water by a modeling fluid having a lower critical pressure and temperature provides a more economical means of performing heat transfer and pressure drop studies.

Entrance-affected, normal and deteriorated heat transfer conditions were defined using CO₂ data from upward flow in an 8 mm diameter tube. For normal heat transfer, the lowest values of

heat-transfer coefficient near the inlet were defined as the threshold values of normal heat transfer. The threshold normal heat-transfer coefficients of the CO₂ data were compared with those of the available water data. The heat-flux-limit relation separating the normal and deteriorated heat transfer was obtained for CO₂ data, and was compared with those for other fluids.

Data were extracted for normal and deteriorated heat transfer from the whole data set. Correlations were then derived separately for normal and deteriorated heat transfer. Using the correlations, the dependence of flow-condition parameters on the heat transfer was examined for different heat transfer modes.

2. HEAT TRANSFER IN SUPERCRITICAL FLUIDS

Heat transfer data for supercritical CO₂ flowing upward in a vertical tube [3] were analysed to examine the normal and deteriorated heat transfer in supercritical flows. The test was performed in the MR-1 loop at AECL, Chalk River Laboratories. The test section consisted of a 2.208 m-long heated section of 8 mm diameter tube. The fluid was heated by means of direct electrical current passing through the tube wall from the inlet to the outlet power terminals. Mixing chambers were installed upstream and downstream of the test section. The mixing chambers increased the mixing of fluid, which made the temperature distribution in the cross-section more uniform. Supercritical CO₂ heat-transfer data were obtained at three pressures above the critical point¹ (7.6, 8.4 and 8.8 MPa), mass fluxes from 900 to 3000 kg m⁻²s⁻¹, heat fluxes up to 600 kW m⁻² and inlet temperatures from 20 to 40°C. Heater (external) surface temperatures were measured with uncertainties of ±0.3°C for the range 0 to 100°C and ±2.2°C for the range beyond 100°C.

2.1 Normal Heat Transfer

Figures 1 to 4 show the heat-transfer coefficient as a function of bulk enthalpy. In each figure, data are presented by the heat flux from the lowest to the highest at similar mass fluxes. The H_{pc} in the figures represents the enthalpy when the bulk temperature is T_{pc} (pseudocritical temperature). Entrance effects on heat transfer are indicated in the figures, where heat transfer shows high values at the inlet. As the flow boundary layer develops, the heat-transfer coefficient exhibits a peak near the H_{pc} ($T_b = T_{pc}$) at low heat fluxes, which is characterized as normal heat transfer. The heat-transfer coefficient peak decreases as the heat flux increases. The reason for enhanced heat transfer at T_{pc} is mainly due to the peak of specific heat (C_p) at T_{pc} .

It is observed in the normal heat-transfer mode that there is an inflection near the inlet, where the value is minimum. At low and intermediate heat fluxes, the minimum heat-transfer coefficients near the inlet are close at similar mass fluxes. The minimum value near the inlet is defined as a threshold value of normal heat transfer, as indicated in Figures 1 to 4.

¹ The critical pressure and temperature of CO₂ are 7.38 MPa and 31.0°C, respectively.

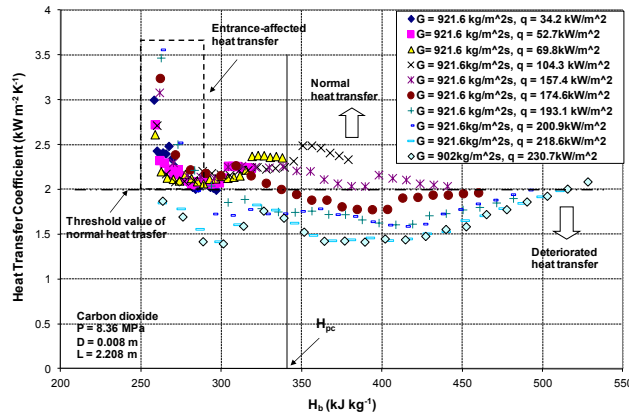


Figure 1: Heat-Transfer Coefficient of CO₂ at Supercritical Pressure 8.36 MPa and Mass Flux 902-922 kg m⁻² s⁻¹

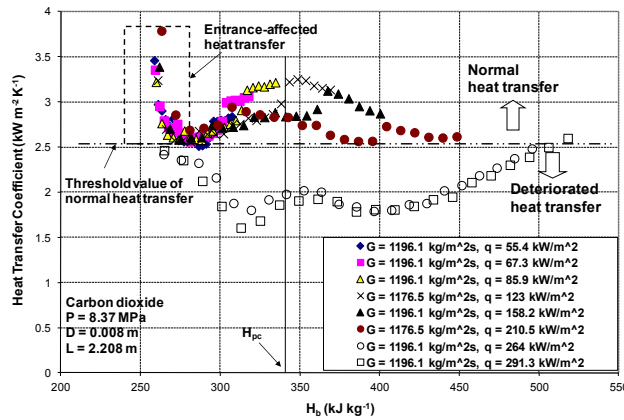


Figure 2: Heat-Transfer Coefficient of CO₂ at Supercritical Pressure 8.37 MPa and Mass Flux 1176-1196 kg m⁻² s⁻¹

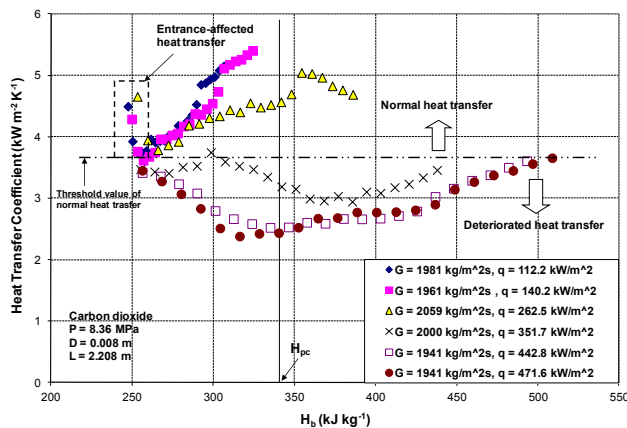


Figure 3: Heat-Transfer Coefficient of CO₂ at Supercritical Pressure 8.36 MPa and Mass Flux 1941-2059 kg m⁻² s⁻¹

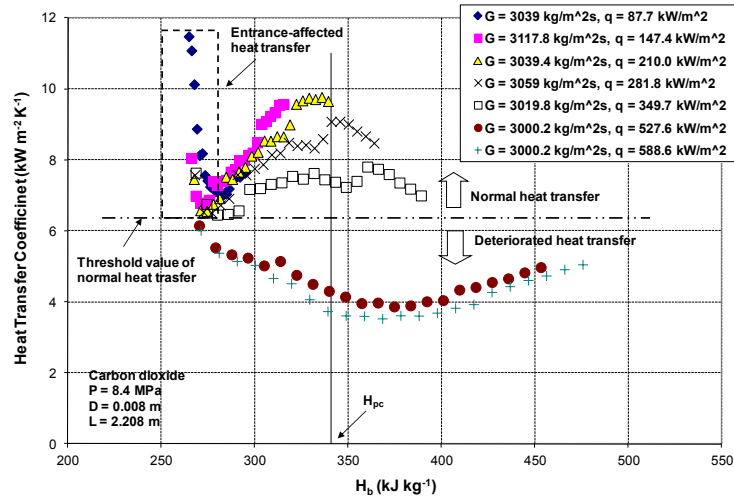


Figure 4: Heat-Transfer Coefficient of CO₂ at Supercritical Pressure 8.4 MPa and Mass Flux 3000-3059 kg m⁻²s⁻¹

Figure 5 shows the effect of mass flux on the threshold normal heat-transfer coefficient (TNHC) for CO₂ upward flow in a vertical tube. The figure also includes the heat flux limit, under which normal heat transfer occurs. The heat flux limit will be explained further in the next section. Figure 5 shows the trend that the TNHC increases as the mass flux increases. Note that the pressure range of the data points in Figure 5 is $P/P_c = 1.13$ to 1.19. Figure 6 compares the threshold values for the present CO₂ data with those of water data from other sources. It is observed that the threshold value of water is higher than that of CO₂ for the given fluid mass flux.

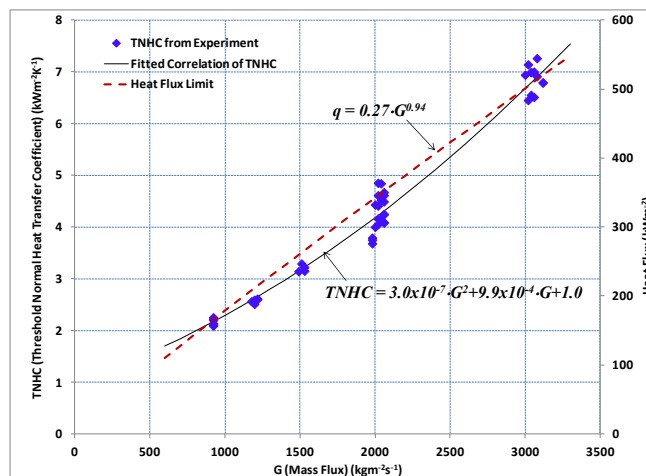


Figure 5: Threshold Normal Heat-Transfer Coefficient of CO₂ at Supercritical Pressure ($P/P_c = 1.13 - 1.19$) (TNHC Denotes Threshold Normal Heat-Transfer Coefficient)

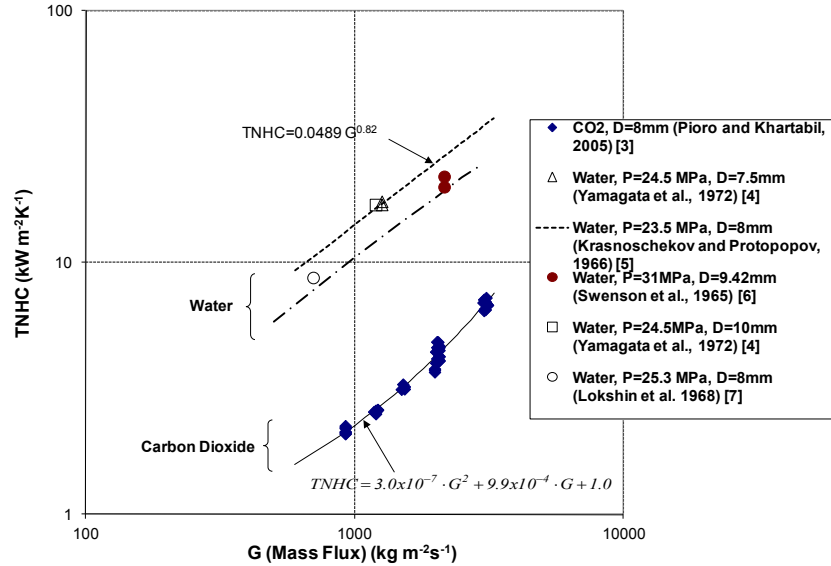


Figure 6: Threshold Normal Heat-Transfer Coefficients of Water and CO₂ at Supercritical Pressure

2.2 Deteriorated Heat Transfer

Beyond a certain heat flux value, this minimum normal heat-transfer coefficient (the threshold value) near the inlet decreases sharply (e.g., $q = 218.6 \text{ kW m}^{-2}$ in Figure 1). Below this threshold normal heat transfer, deteriorated heat transfer occurs. Jackson and Hall [8] suggested that the dominant factor for deteriorated heat transfer was the result of the modification of the shear stress near the wall. As the wall temperature increases, the density decreases in the boundary near the heated surface. This causes a buoyancy force due to a reduced density, which acts in the direction of motion leading to a reduction of the shear stress near the wall. As a result, the turbulent kinetic energy decreases, and turbulent diffusivity decreases.

The change from normal to deteriorated heat transfer depends on heat flux and mass flux. For supercritical water, Yamagata *et al.* [4] proposed a relation of the heat flux limit for vertically upward flow.

$$q = 0.20 \cdot G^{1.2} \quad (1)$$

where q is heat flux in kW m^{-2} and G is mass flux in $\text{kg m}^{-2}\text{s}^{-1}$. A heat flux factor for water (K_w) can be defined to differentiate the heat transfer mode as:

$$K_w = \frac{q}{G^{1.2}} \quad (2)$$

Note that K_w is dimensional. The mode of heat transfer is normal when $K_w \leq 0.2$, and deteriorated when $K_w > 0.2$.

In this study, the heat flux limit relation of CO₂ was obtained after examining the CO₂ data with normal and deteriorated heat transfer.

$$q = 0.27 G^{0.94} \quad (3)$$

Similar to water, a heat flux factor for CO₂ (K_c) is defined as:

$$K_c = \frac{q}{G^{0.94}} \quad (4)$$

The mode of heat transfer is normal when $K_w \leq 0.27$, and deteriorated when $K_w > 0.27$. For each test run, heat transfer along the length of the test section can be differentiated into normal or deteriorated heat transfer by the heat flux factor (refer to Figures 1 to 4 for CO₂ data). For CO₂, a heat flux factor greater than 0.27 indicates deteriorated heat transfer.

For deteriorated heat transfer in Figures 1 to 4, the heat-transfer coefficient decreases as the heat flux increases. At low mass flux (Figures 1 to 3), the heat-transfer coefficient distribution shows a typical shape of “W”. The “W” shape becomes widened as the mass flux increases.

Figure 7 shows deteriorated heat-transfer data including the heat flux limit lines for CO₂. The data and the heat flux limit line for water and helium are also included in the Figure for comparison. The water heat flux line is located higher than the CO₂ heat flux line. The figure also implies that the heat flux limit of water, CO₂ and helium can be explained in a similar way.

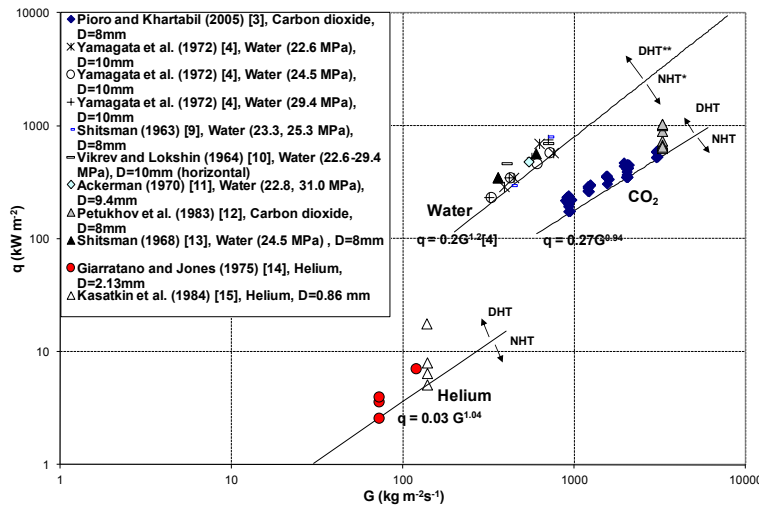


Figure 7: Mass Flux and Heat Flux in Deteriorated Heat Transfer Showing the Limit Criteria of Normal Heat Transfer in Supercritical Water, CO₂ and Helium (NHT*: Normal Heat Transfer, DHT: Deteriorated Heat Transfer)**

3. CORRELATIONS FOR NORMAL AND DETERIORATED HEAT TRANSFER

3.1 Derivation of Correlations

The approach in this study was to derive correlations that contain relevant dimensionless parameters using the available CO₂ data, and to examine the effect of flow condition parameters

on heat transfer for different heat-transfer modes. A number of dimensionless groups available in existing correlations were tested to find the appropriate correlation form representing the CO₂ data. The correlations were derived by including additional similarity groups to the form of the Petukhov *et al.* [16] correlation. The form of the present correlations is:

$$Nu_b = a \left(\frac{P}{P_c} \right)^b \left(\frac{T_b}{T_{pc}} \right)^c \left(10000 \frac{q}{GH_b} \right)^d (Nu_0)^e \left(\frac{\mu_b}{\mu_w} \right)^f \left(\frac{k_b}{k_w} \right)^g \left(\frac{C_p}{C_{pb}} \right)^h \quad (5)$$

where

$$Nu_b = \frac{hD}{k_b} \quad \text{or} \quad \frac{qD}{k(T_w - T_b)}$$

$$Nu_0 = \frac{\frac{C_f}{2} Re_b Pr_b}{12.7 \left(\frac{C_f}{2} \right)^{1/2} (Pr_b^{2/3} - 1) + 1.07}$$

$$Re_b = \frac{GD}{\mu_b}$$

$$Pr_b = \frac{C_{pb} \mu_b}{k_b}$$

$$C_f = \frac{1}{(3.64 \log Re_b - 3.28)^2}$$

The correlation was derived separately for normal and deteriorated heat transfer. For normal heat transfer, entrance-affected data, which are specific to the configuration at the inlet, were excluded in deriving the correlation. The correlation for normal heat transfer was fitted using 1416 data points for CO₂. The coefficient and exponents of the correlation are included in Table 1. The data were correlated with an average error of -0.22% and an RMS error of 10.33%. The data used in the correlation cover the range of dimensionless parameters listed in Table 2.

For deteriorated heat transfer, data affected by the entrance were likewise excluded. Data in the outlet region, whose values were above the threshold value, were also excluded. The 1172 data points of CO₂ were used in deriving the correlation. The coefficient and exponents of the correlation are included in Table 1. The correlation was fitted with an average error of -0.56 % and an RMS error of 6.91 %. The range of dimensionless parameters in the correlation is listed in Table 2.

The correlations for different heat-transfer modes represent the dependence of the dimensionless parameters on the Nusselt number (Nu_b). The exponent (0.13205) in the correlation of the heat flux parameter (q/GH_b) of normal heat transfer is a positive value, which means that the Nusselt number increases as the heat flux parameter increases. The exponent (-0.32562) of the heat flux

parameter of deteriorated heat transfer is a negative value, which indicates that the parameter affects the Nusselt number in the opposite way, compared to normal heat transfer. The viscosity and thermal conductivity parameters have also opposite effects on the Nusselt number, which may be due to the difference of flow structure between two different heat transfer modes.

Table 1
Coefficient and Exponents of the Correlation

	a	b	c	d	e	f	g	h
Normal Heat Transfer	0.41179	-0.43274	1.84087	0.13205	1.10223	-0.92839	0.16801	0.72487
Deteriorated Heat Transfer	1.7065	-0.53838	2.46823	-0.32562	0.94871	0.50388	-0.54941	0.57156

Table 2
Range of Dimensionless Parameters of the Correlations

	$\frac{P}{P_c}$	$\frac{T_b}{T_{pc}}$	$10000 \frac{q}{GH_b}$	Nu_0	$\frac{\mu_b}{\mu_w}$	$\frac{k_b}{k_w}$	$\frac{\overline{C_p}}{C_{pb}}$
Normal Heat Transfer	1.03 ~ 1.20	0.95~ 1.22	0.98 ~ 5.78	416 ~ 4329	0.92 ~ 3.47	0.92 ~ 4.25	0.05 ~ 2.22
Deteriorated Heat Transfer	1.03 ~ 1.21	0.95 ~ 1.25	3.49 ~ 9.67	395 ~ 4518	0.82 ~ 3.36	0.80 ~ 4.25	0.01 ~ 0.92

3.2 Prediction with Correlations

Figures 8 and 9 show comparisons of the CO₂ data [3] with the fitted correlation for normal heat transfer. The present correlation fits the data with good accuracy. Predictions of the CO₂ data with other correlations are included for comparison. In general, other correlations applied in this study over-predicted the CO₂ data. The Swenson et al. (1965) [6] shows the closest prediction to the data among the other correlations.

Figures 10 and 11 show comparisons of the CO₂ data with the fitted correlation for deteriorated heat transfer. The fitted correlation fits the data, and also the typical “W” shape, reasonably well. Figure 12 presents the prediction of other CO₂ data (Petukhov et al. 1983) [12] with the present correlation for deteriorated heat transfer. The prediction exhibits a good agreement with the data.

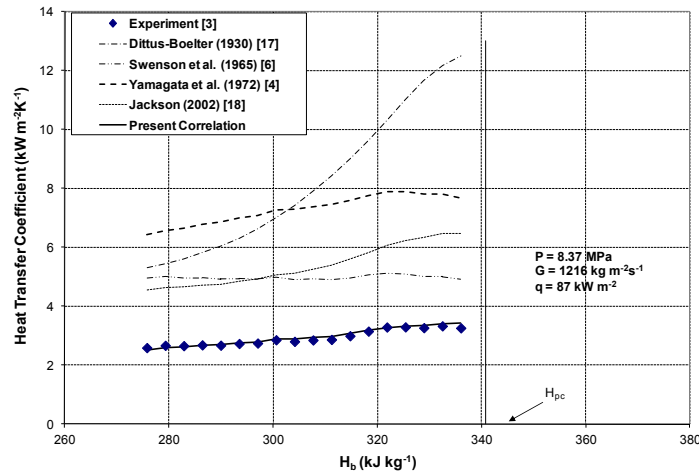


Figure 8: Comparison of the CO₂ Data with the Fitted Correlation and Prediction of the CO₂ Data with Other Correlations for Normal Heat Transfer

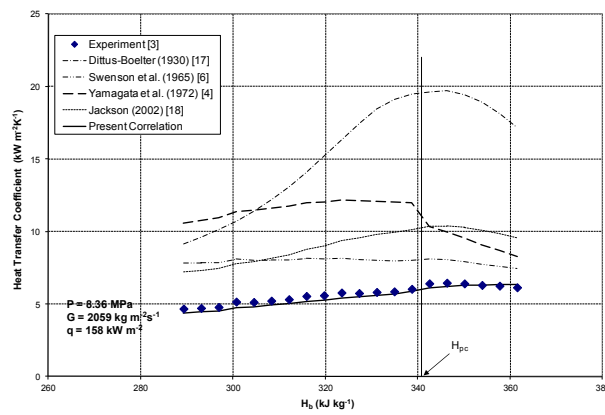


Figure 9: Comparison of the CO₂ Data with the Fitted Correlation and Prediction of the CO₂ Data with Other Correlations for Normal Heat Transfer

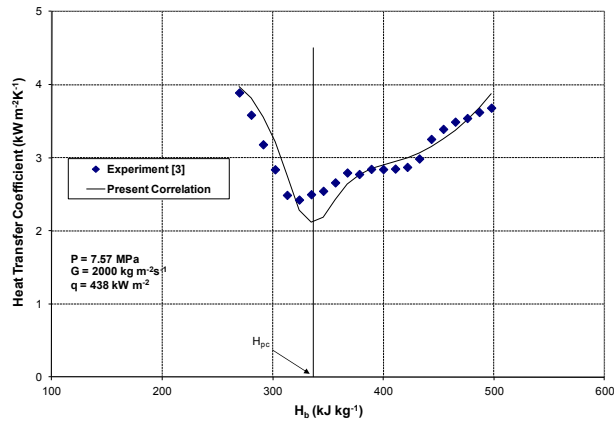


Figure 10: Comparison of CO₂ Data with the Fitted Correlation for Deteriorated Heat Transfer

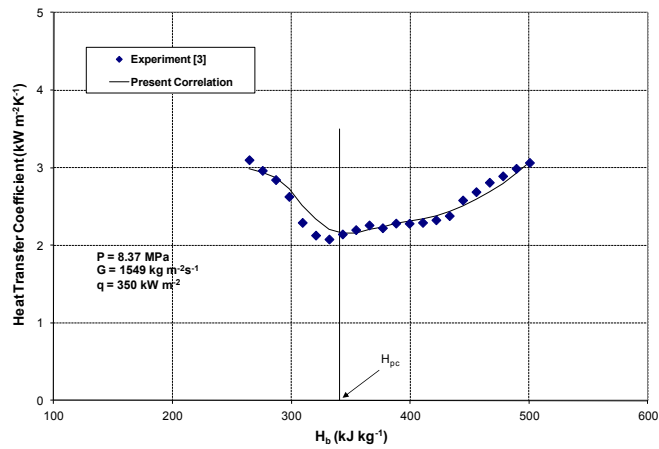


Figure 11 – Comparison of CO₂ Data with the Fitted Correlation for Deteriorated Heat Transfer

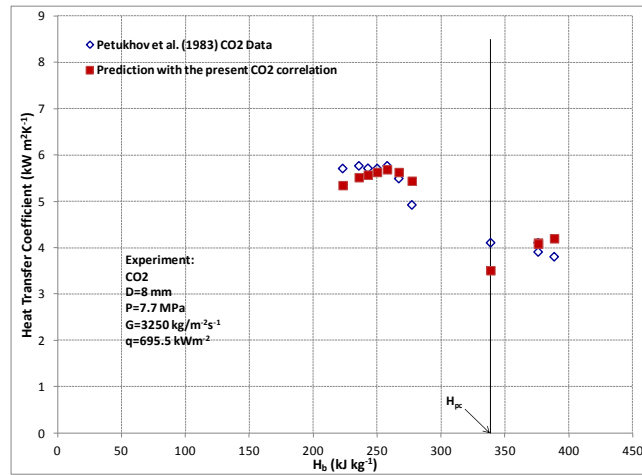


Figure 12 – Prediction of Petukhov et al. (1983) [12] CO₂ Data with the Present Correlation for Deteriorated Heat Transfer

4. CONCLUSIONS

Heat-transfer modes in supercritical fluids were examined using the heat-transfer data for supercritical CO₂ flowing upward in a 8 mm tube. The following conclusions are made:

- Normal and deteriorated heat-transfer phenomena of CO₂ at supercritical pressure were identified by examining the CO₂ data. The threshold value represented by the minimum value of normal heat transfer was identified, showing a consistent trend in that the threshold value increases as the mass flux increases.
- The heat flux limit relation dividing normal and deteriorated heat transfer for upward CO₂ flow in a 8 mm tube was found to be $q = 0.27 G^{0.94}$, where q is in kW/m² and G is in kg/m²s.
- The approach in this study was to derive correlations that contain relevant dimensionless parameters using available CO₂ data, and to examine the dependence of parameter on heat-transfer coefficient for different heat-transfer modes. Dimensionless correlations were derived separately for normal and deteriorated heat transfer. The correlation for normal heat transfer was fitted with an average error of 0.22% and an RMS error of 10.3%. The data for deteriorated heat transfer were correlated with an average error of -0.56% and an RMS error of 6.91%.
- Comparisons of the derived correlations showed good agreement with the fitted CO₂ data. The correlations derived using CO₂ data presented the effect of flow condition parameters on heat transfer for different heat-transfer modes.

5. NOMENCLATURE

<u>Symbol</u>	<u>Description</u>	<u>unit</u>
C_p	Specific heat at constant pressure	J/kg K
$\overline{C_p}$	Average specific heat, $\overline{C_p} = (H_w - H_b)/(T_w - T_b)$	J/kg K
D	Inside Diameter of Tube	m

G	Mass Flux	$\text{kg/m}^2\text{s}$
h	Heat-Transfer Coefficient	$\text{W/m}^2\text{K}$
H	Enthalpy	J/kg
k	Thermal Conductivity	W/mK
K_c	Heat Flux Factor of CO_2	as defined in Eq. (4)
K_w	Heat Flux Factor of Water	as defined in Eq. (2)
Nu	Nusselt Number, $Nu = hD/k$	—
P	Pressure	kPa
Pr	Prandtl Number, $Pr = \mu C_p / k$	—
\overline{Pr}	Average Prandtl Number, $\overline{Pr} = \mu \overline{C_p} / k$	—
q	Wall Heat Flux	W/m^2
Re	Reynolds Number, $Re = GD/\mu$	—
T	Temperature	K
Greek		
μ	Dynamic Viscosity of Fluid	kg/ms
Subscripts		
b	at bulk temperature, T_b	
c	at critical condition	
o	refers to reference	
p	at constant temperature	
pc	at pseudocritical condition	
w	at wall temperature, T_w	

6. REFERENCES

- [1] L.K.H. Leung, M. Yetisir, W. Diamond, D. Martin, J. Pencer, B. Hyland, H. Hamilton, D. Guzonas and R. Duffey, "A next generation heavy water nuclear reactor with supercritical water as coolant", International Conference of Future of Heavy Water Reactors, Paper 042, Ottawa, Ontario, Canada, 2011 October 02-05
- [2] S.K. Yang and H.F. Khartabil, "Normal and deteriorated heat transfer correlations for supercritical fluids", Transactions of the American Nuclear Society, ANS 2009 Winter Meeting, Vol. 93, pp. 635-637, Washington, D.C., USA, 2005 November 13-17.

- [3] I.L. Pioro and H.F. Khartabil, "Experimental study on heat transfer to supercritical carbon dioxide flowing upward in a vertical tube," 13th Int. Conf. On Nuclear Engineering (ICONE-13), Beijing, China, Paper-50118, 2005 May 16-20.
- [4] K. Yamagata, K. Nishikawa, S. Hasegawa, T. Fujii and S. Yoshida, "Forced convective heat transfer to supercritical water flowing in tubes", *International Journal of Heat and Mass Transfer*, 15 (12), pp. 2575-2593, 1972.
- [5] A. Krasnoshchekov and V.S. Protopopov, "Experimental study of heat exchanger in carbon dioxide in the supercritical range at high temperature drops", *High Temperatures*, 4 (3), pp. 375-382, 1966.
- [6] H.S. Swenson, J.R. Carver and C.R. Kakarala, "Heat transfer to supercritical water in smooth-bore tubes", *Journal of Heat Transfer, Transactions of the ASME*, Series C, 87 (4), pp. 477-484, 1965.
- [7] V.A. Lokshin, I.E. Semenovker and V. Vikhrev, "Calculating the temperature conditions of the radiant heating surfaces in supercritical boilers", *Thermal Engineering*, 15 (9), pp. 34-39, 1968.
- [8] J.D. Jackson and W.B. Hall, "Forced convection heat transfer to fluids at supercritical pressure" in *Turbulent Forced Convection in Channels and Bundles*, Editors, S. Kakac and D.B. Spalding, Hemisphere Corp., New York, New York, USA, Vol. 2, pp. 563-612, 1979.
- [9] M.E. Shitsman, "Impairment of the heat transmission at supercritical pressures", *High Temperatures*, 1 (2), pp. 237-244, 1963.
- [10] Yu.V. Vikrev and V.A. Lokshin, "An Experimental Study of Temperature Conditions in Horizontal Steam-Generating Tubes at Supercritical Pressures", *Thermal Engineering*, 11 (12), pp. 105-109, 1964.
- [11] J.W. Ackerman, "Pseudoboiling heat transfer to supercritical pressure water in smooth and ribbed tubes", *Journal of Heat Transfer, Transactions of the ASME*, 92 (3), pp. 490-498 (Paper No. 69-WA/HT-2, pp. 1-8), 1970.
- [12] B.S. Petukhov, V.A. Kurganov and V.B. Ankudinov, "Heat transfer and flow resistance in the turbulent pipe flow of a fluid with near-critical state parameters", *High Temperatures*, 21 (1), pp. 81-89, 1983.
- [13] M.E. Shitsman, "Temperature conditions in tubes at supercritical pressures", *Thermal Engineering*, 15 (5), pp. 72-77, 1968.
- [14] P.J. Giarratano and M.C. Jones, "Determination of heat transfer to supercritical helium at 2.5 atmospheres", *International Journal of Heat and Mass Transfer*, 18 (5), pp. 649-653, 1975.

- [15] A.P. Kasatkin, D.A. Labuntsov and R.I. Soziev, “An experimental investigation of heat transfer with turbulent flow of helium at supercritical parameters of state”, *Thermal Engineering*, 31 (10), pp. 578-580, 1984.
- [16] B.S. Petukhov, E.A. Krasnoschekov and V.S. Protopopov, “An investigation of heat transfer to fluids flowing in pipes under supercritical conditions”, International Developments in Heat Transfer: Proc. 1961-1962, Papers presented at the 1961 International Heat Transfer Conf., ASME, University of Colorado, Boulder, U.S.A., Part III, Paper 6, pp. 569-578, 1961.
- [17] F.W. Dittus and L.M.K. Boelter, “Heat transfer in automobile radiators of tubular type”, University of California, Berkeley, Publications in *Engineering*, 2 (13), pp. 443-461, 1930.
- [18] J.D. Jackson, “Consideration of the heat transfer properties of supercritical pressure water in connection with the cooling of advanced nuclear reactors”, Proceedings of the 13th Pacific Basin Nuclear Conference, Shenzhen City, China, 2002 October 21-25.